

# Classification of Schizophrenia from Functional MRI Using Large-scale Extended Granger Causality

Axel Wismüller,<sup>a,b,c,d</sup> and M. Ali Vosoughi<sup>a</sup>

<sup>a</sup>Department of Electrical and Computer Engineering, University of Rochester, NY, USA

<sup>b</sup>Department of Imaging Sciences, University of Rochester, NY, USA

<sup>c</sup>Department of Biomedical Engineering, University of Rochester, NY, USA

<sup>d</sup>Faculty of Medicine and Institute of Clinical Radiology, Ludwig Maximilian University, Munich, Germany

## ABSTRACT

The literature manifests that schizophrenia is associated with alterations in brain network connectivity. We investigate whether large-scale Extended Granger Causality (lsXGC) can capture such alterations using resting-state fMRI data. Our method utilizes dimension reduction combined with the augmentation of source time-series in a predictive time-series model for estimating directed causal relationships among fMRI time-series. The lsXGC is a multivariate approach since it identifies the relationship of the underlying dynamic system in the presence of all other time-series. Here lsXGC serves as a biomarker for classifying schizophrenia patients from typical controls using a subset of 62 subjects from the Centers of Biomedical Research Excellence (COBRE) data repository. We use brain connections estimated by lsXGC as features for classification. After feature extraction, we perform feature selection by Kendall's tau rank correlation coefficient followed by classification using a support vector machine. As a reference method, we compare our results with cross-correlation, typically used in the literature as a standard measure of functional connectivity. We cross-validate 100 different training/test (90%/10%) data split to obtain mean accuracy and a mean Area Under the receiver operating characteristic Curve (AUC) across all tested numbers of features for lsXGC. Our results demonstrate a mean accuracy range of [0.767, 0.940] and a mean AUC range of [0.861, 0.983] for lsXGC. The result of lsXGC is significantly higher than the results obtained with the cross-correlation, namely mean accuracy of [0.721, 0.751] and mean AUC of [0.744, 0.860]. Our results suggest the applicability of lsXGC as a potential biomarker for schizophrenia.

---

Further author information: (Send correspondence to Ali Vosoughi)

Ali Vosoughi: E-mail: mvosough@ur.rochester.edu

**Keywords:** machine learning, resting-state fMRI, Granger causality, functional connectivity, feature space, schizophrenia disorder

## 1. INTRODUCTION

Schizophrenia is a psychiatric disorder characterized by thoughts or experiences that are out of touch with reality, decreased participation in daily activities, disorganized speech or behavior, and (probably) difficulty with concentration and memorization may also be present. The current diagnosis of schizophrenia is by using clinical evaluations of symptoms and behaviors; nevertheless, measurable biomarkers can be beneficial. Recent studies on brain imaging data have shown that information can be extracted non-invasively from brain activity. Despite these studies' promising results, there is still scope for improvement, especially using more meaningful connectivity analysis approaches [1].

Extensive evidence has demonstrated that schizophrenia affects the brain's connectivity [2]. Biomarkers from resting-state functional MRI (rs-fMRI) for schizophrenia can be derived using Multi-Voxel Pattern Analysis (MVPA) techniques [3]. MVPA is a framework based on pattern recognition that extracts differences in brain connectivity patterns among healthy individuals and individuals with neurological disease. Cross-correlation is commonly used in most MVPA studies to obtain a functional connectivity profile. For instance, one such study has obtained an accuracy of 0.79 on the slow frequency bands (0.01-0.1 Hz) [4]. As a result, one can argue that connectivity analysis of fMRI data can be used to learn meaningful information. However, cross-correlation is not fit to obtain directed measures of connectivity. Therefore, there may be more relevant information in the fMRI data that is not being grasped by cross-correlation. Several methods have been proposed to capture directional relations in multivariate time-series data, e.g., transfer entropy [5] and mutual information [6]. However, as the multivariate problem's dimensions increase, the density function's computation becomes computationally expensive [7,8]. Under the Gaussian assumption, transfer entropy is equivalent to Granger causality [9]. However, the computation of multivariate Granger causality for short time series in large-scale problems is challenging [10,11].

Large-scale Extended Granger Causality (lsXGC) is a recently proposed method for estimating directed causal relationships among fMRI time-series that combines dimension reduction with source time-series augmentation and uses predictive time-series modeling [12]. In this work, we investigate if alterations in directed connectivity evident in individuals with schizophrenia and if such directed measures enhance our ability to discriminate between schizophrenia patients and healthy controls. To this end, we apply lsXGC in the MVPA framework for estimating a measure of directed causal interdependence between fMRI time-series.

This work is embedded in our group's endeavor to expedite artificial intelligence in biomedical imaging by means

of advanced pattern recognition and machine learning methods for computational radiology and radiomics, e.g., [13–70].

## 2. DATA

### 2.1 Participants

The Centers of Biomedical Research Excellence (COBRE) data respiratory contains raw anatomical and functional MR data from 72 patients with schizophrenia and 74 healthy controls (ages ranging from 18 to 65 in each group). All subjects were screened and eliminated if they had; a history of mental retardation, a history of neurological disorder, history of severe head trauma with more than 5 minutes of loss of consciousness, history of substance dependence or abuse within the last 12 months [2]. Diagnostic information was collected using the Structured Clinical Interview used for DSM Disorders (SCID) [2].

### 2.2 Resting-state fMRI data

A multi-echo MPRAGE (MEMPR) sequence was used with the following parameters: TR/TE/TI = 2530/[1.64, 3.5, 5.36, 7.22, 9.08]/900 ms, flip angle = 7°, FOV = 256 x 256 mm<sup>2</sup>, slab thickness = 176 mm, matrix = 256 x 256 x 176, voxel size = 1 x 1 x 1 mm<sup>3</sup>, number of echos = 5, pixel bandwidth = 650 Hz, total scan time = 6 min. With 5 echoes, the TR, TI and time to encode partitions for the MEMPR are similar to that of a conventional MPRAGE, resulting in similar GM/WM/CSF contrast. Resting-state fMRI data was collected with single-shot full k-space echo-planar imaging (EPI) with ramp sampling correction using the intercommissural line (AC-PC) as a reference (TR = 2 s, TE = 29 ms, matrix size = 64 x 64, 32 slices, voxel size = 3 x 3 x 4 mm<sup>3</sup>).

Functional connectivity measurements were generated from a subsample of the COBRE dataset [71], a publicly available sample which we accessed through the Nilearn Python library [72]. All subjects of healthy controls and diseased patients under the age of 32 were selected, including 33 healthy and 29 diseased subjects, totaling 62 individuals. The images were already preprocessed using the NIAK resting-state pipeline [73], and additional details can be found in the reference [71]. The number of regions of interests has been selected to be 122 with functional brain parcellations [74].

## 3. METHODS

### 3.1 Large-scale Extended Granger Causality (lsXGC)

The Large-scale Extended Granger Causality (lsXGC) method has been developed based on 1) the principle of original Granger causality that quantifies the causal influence of time-series  $\mathbf{x}_s$  on time-series  $\mathbf{x}_t$  by quantifying the measure of improvement in the forecast of  $\mathbf{x}_t$  in the presence of  $\mathbf{x}_s$ . 2) the idea of dimensionality reduction,

which solves the problem of tackling an ill-posed system, which is often challenged in fMRI analysis since the number of acquired temporal samples usually is not sufficient for estimating the model parameters [10, 65].

Consider the ensemble of time-series  $\mathcal{X} \in \mathbb{R}^{N \times T}$ , where  $N$  is the regions of interest (ROIs or number) of time-series and  $T$  the number of temporal samples. Let  $\mathcal{X} = (\mathbf{x}_1, \mathbf{x}_2, \dots, \mathbf{x}_N)^\top$  be the whole multidimensional system and  $x_i \in \mathbb{R}^{1 \times T}$  a single time-series with  $i = 1, 2, \dots, N$ , where  $\mathbf{x}_i = (x_i(1), x_i(2), \dots, x_i(T))$ . To overcome the ill-posed problem, first  $\mathcal{X}$  will be decomposed into its first  $p$  high-variance principal components  $\mathcal{Z} \in \mathbb{R}^{p \times T}$  using Principal Component Analysis (PCA), i.e.,

$$\mathcal{Z} = W\mathcal{X}, \quad (1)$$

where  $W \in \mathbb{R}^{p \times N}$  represents the PCA coefficient matrix. Subsequently, the dimension-reduced time-series ensemble  $\mathcal{Z}$  is augmented by one original time-series  $\mathbf{x}_s$  yielding a dimension-reduced augmented time-series ensemble  $\mathcal{Y} \in \mathbb{R}^{(p+1) \times T}$  for estimating the influence of  $\mathbf{x}_s$  on all other time-series.

Following this, we locally predict  $\mathcal{X}$  at each time sample  $t$ , i.e.,  $\mathcal{X}(t) \in \mathbb{R}^{N \times 1}$  by calculating an estimate  $\hat{\mathcal{X}}_{\mathbf{x}_s}(t)$ . To this end, we fit an affine model based on a vector of  $m$  vector of  $m$  time samples of  $\mathcal{Y}(\tau) \in \mathbb{R}^{(p+1) \times 1}$  ( $\tau = t-1, t-2, \dots, t-m$ ), which is  $\mathbf{y}(t) \in \mathbb{R}^{m \cdot (p+1) \times 1}$ , and a parameter matrix  $\mathcal{A} \in \mathbb{R}^{N \times m \cdot (p+1)}$  and a constant bias vector  $\mathbf{b} \in \mathbb{R}^{N \times 1}$ ,

$$\hat{\mathcal{X}}_{\mathbf{x}_s}(t) = \mathcal{A}\mathbf{y}(t) + \mathbf{b}, \quad t = m+1, m+2, \dots, T. \quad (2)$$

Now  $\hat{\mathcal{X}}_{\setminus \mathbf{x}_s}(t)$ , which is the prediction of  $\mathcal{X}(t)$  without the information of  $\mathbf{x}_s$ , will be estimated. The estimation processes is identical to the previous one, with the only difference being that we have to remove the augmented time-series  $\mathbf{x}_s$  and its corresponding column in the PCA coefficient matrix  $W$ .

The computation of a lsXGC index is based on comparing the variance of the prediction errors obtained with and without consideration of  $\mathbf{x}_s$ . The lsXGC index  $f_{\mathbf{x}_s \rightarrow \mathbf{x}_t}$ , which indicates the influence of  $\mathbf{x}_s$  on  $\mathbf{x}_t$ , can be calculated by the following equation:

$$f_{\mathbf{x}_s \rightarrow \mathbf{x}_t} = \log \frac{\text{var}(e_s)}{\text{var}(e_{\setminus s})}, \quad (3)$$

where  $e_{\setminus s}$  is the error in predicting  $\mathbf{x}_t$  when  $\mathbf{x}_s$  was not considered, and  $e_s$  is the error, when  $\mathbf{x}_s$  was used. In this study, we set  $p = 8$  and  $m = 1$ .

### 3.2 Multi-voxel pattern analysis

Brain connections served as features for classification in this study and were estimated by two methods, namely lsXGC and cross-correlation. Before using high-dimensional connectivity feature vectors as input to a classifier, feature selection was carried out to reduce input features' dimension.

### 3.2.1 Feature selection

In order to lessen the number of features, feature selection was performed on each training data set with k-fold cross-validation using *Kendall's Tau* rank correlation coefficient [75] and 10% – 90% of test-to-train split ratio. This approach quantifies each feature's relevance to the task of classification and assigns ranks by testing for independence between different classes for each feature [75].

### 3.2.2 Classification

To cross-validate the classification performance in 100 iterations, the data set was divided into two groups: a training data set (90%) and a test data set (10%) that the percentage of samples for each class was preserved. Also, this was repeated with different numbers of features ranging from 5 to 175. A Support Vector Machine (SVM) [76] was used for classification between healthy subjects and schizophrenia patients. All procedures were performed using MATLAB 9.8 (MathWorks Inc., Natick, MA, 2020a), and Python 3.8.

## 4. RESULTS

Mean connectivity matrices, which were extracted using lsXGC and cross-correlation, are shown in Fig. 1 for schizophrenia patient and healthy control cohorts. Distinct patterns are visible to the naked eye for both methods. In the following, we quantitatively investigate the difference between the two patient cohorts' connectivity patterns using an MVPA approach.

Classification results were evaluated using the Area Under the Receiver Operator Characteristic Curve (AUC) and accuracy. An  $AUC = 1$  indicates a perfect classification,  $AUC = 0.5$  indicates random class assignment. In this study, we chose eight as the number of the retained components of PCA in the lsXGC algorithm and model order of 1 for the multivariate vector autoregression function based on preliminary analyses. The plots of accuracy and AUC results in Fig. 2, clearly demonstrate that lsXGC outperforms cross-correlation for diversified numbers of features. Across the wide range of examined numbers of features, the performance of lsXGC is consistently higher with its mean AUC within [0.861, 0.983] and its mean accuracy within [0.767, 0.940]. On the other hand, cross-correlation performs quite poorly compared to lsXGC with its mean AUC within [0.744, 0.860] and its mean accuracy within [0.721, 0.751].

## 5. CONCLUSIONS

In this research, we use a recently developed method for brain connectivity analysis, large-scale Extended Granger Causality (lsXGC), and apply it to a subset of the COBRE data repository to classify individuals with schizophrenia from typical controls by estimating a measure of directed causal relations among regional brain activities

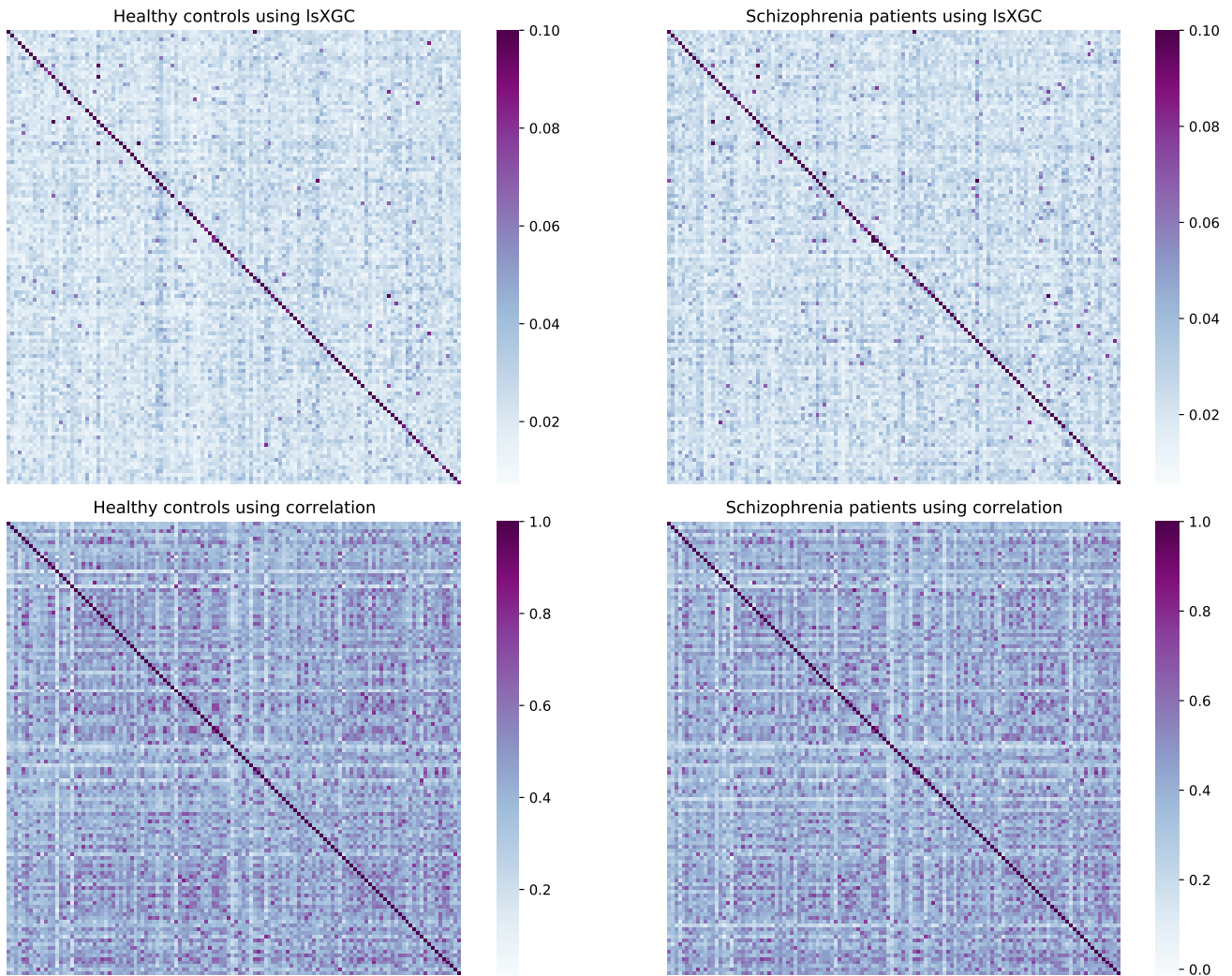


Figure 1: Mean connectivity matrices: top left: mean connectivity of healthy control subjects using lsXGC, top right: mean connectivity matrix of schizophrenia patients using lsXGC, bottom left: mean connectivity matrix of healthy control subjects using cross-correlation, bottom right: employing cross-correlation to obtain mean connectivity matrix of schizophrenia patients. Remarkably different methods appear to extract different connectivity features, and that they appear to be slight differences in connectivity patterns between the healthy subject and the schizophrenia patients.

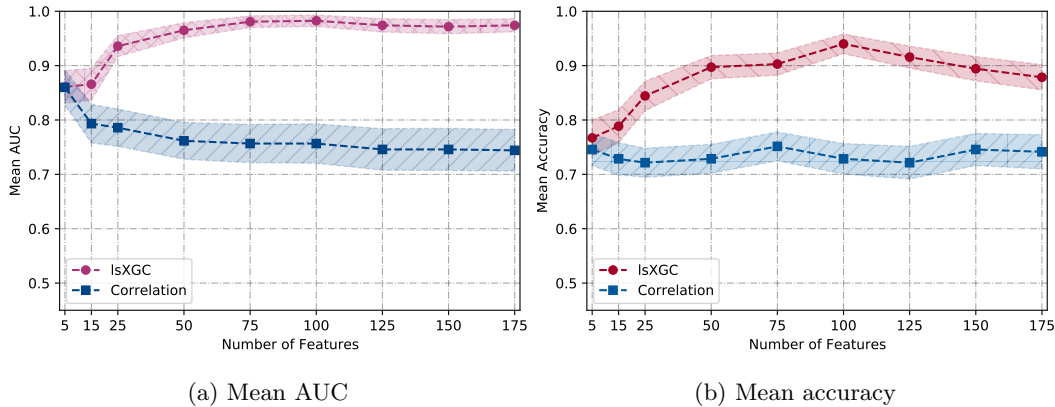


Figure 2: Plots are comparing the performance of cross-correlation and the proposed large-scale extended Granger causality (lsXGC). The shaded areas represent the 95% confidence interval. It demonstrates that lsXGC outperforms cross-correlation for most numbers of selected features.

recorded in resting-state fMRI. Following the construction of connectivity matrices as characterizing features for brain network analysis, we use Kendall’s tau rank correlation coefficient to select a significant feature and a support vector machine to classify. We demonstrate that our method (lsXGC) favorably compares to standard analysis using cross-correlation, as shown by the significantly enhancing accuracy and AUC values. The effectiveness of lsXGC as a potent biomarker for identifying schizophrenia in prospective clinical trials is yet to be validated. Nevertheless, our results suggest that our approach outperforms the current clinical standard, namely cross-correlation, at revealing meaningful information from functional MRI data.

## ACKNOWLEDGMENTS

This research was funded by Ernest J. Del Monte Institute for Neuroscience Award from the Harry T. Mangurian Jr. Foundation. This work was conducted as a Practice Quality Improvement (PQI) project related to American Board of Radiology (ABR) Maintenance of Certificate (MOC) for Prof. Dr. Axel Wismüller. This work is not being and has not been submitted for publication or presentation elsewhere.

## REFERENCES

- [1] Li, A., Zalesky, A., Yue, W., Howes, O., Yan, H., Liu, Y., Fan, L., Whitaker, K. J., Xu, K., Rao, G., et al., “A neuroimaging biomarker for striatal dysfunction in schizophrenia,” *Nature Medicine* **26**(4), 558–565 (2020).
- [2] Calhoun, V. D., Sui, J., Kiehl, K., Turner, J. A., Allen, E. A., and Pearlson, G., “Exploring the psychosis functional connectome: aberrant intrinsic networks in schizophrenia and bipolar disorder,” *Frontiers in psychiatry* **2**, 75 (2012).

- [3] Norman, K. A., Polyn, S. M., Detre, G. J., and Haxby, J. V., “Beyond mind-reading: multi-voxel pattern analysis of fMRI data,” *Trends in cognitive sciences* **10**(9), 424–430 (2006).
- [4] Cheng, H., Newman, S., Goñi, J., Kent, J. S., Howell, J., Bolbecker, A., Puce, A., O’Donnell, B. F., and Hetrick, W. P., “Nodal centrality of functional network in the differentiation of schizophrenia,” *Schizophrenia research* **168**(1-2), 345–352 (2015).
- [5] Schreiber, T., “Measuring information transfer,” *Physical review letters* **85**(2), 461 (2000).
- [6] Kraskov, A., Stögbauer, H., and Grassberger, P., “Estimating mutual information,” *Physical review E* **69**(6), 066138 (2004).
- [7] Mozaffari, M. and Yilmaz, Y., “Online multivariate anomaly detection and localization for high-dimensional settings,” *arXiv preprint arXiv:1905.07107* (2019).
- [8] Mozaffari, M. and Yilmaz, Y., “Online anomaly detection in multivariate settings,” in [*2019 IEEE 29th International Workshop on Machine Learning for Signal Processing (MLSP)*], 1–6, IEEE (2019).
- [9] Barnett, L., Barrett, A. B., and Seth, A. K., “Granger causality and transfer entropy are equivalent for Gaussian variables,” *Physical review letters* **103**(23), 238701 (2009).
- [10] Vosoughi, M. A. and Wismüller, A., “Large-scale kernelized Granger causality to infer topology of directed graphs with applications to brain networks,” *arXiv preprint arXiv:2011.08261* (2020).
- [11] Wismüller, A., DSouza, A. M., Abidin, A. Z., and Vosoughi, M. A., “Large-scale nonlinear Granger causality: A data-driven, multivariate approach to recovering directed networks from short time-series data,” *arXiv preprint arXiv:2009.04681* (2020).
- [12] Vosoughi, M. A. and Wismüller, A., “Large-scale extended Granger causality for classification of marijuana users from functional MRI,” *arXiv preprint arXiv:2101.01832* (2021).
- [13] Nattkemper, T. W. and Wismüller, A., “Tumor feature visualization with unsupervised learning,” *Medical Image Analysis* **9**(4), 344–351 (2005).
- [14] Bunte, K., Hammer, B., Wismüller, A., and Biehl, M., “Adaptive local dissimilarity measures for discriminative dimension reduction of labeled data,” *Neurocomputing* **73**(7-9), 1074–1092 (2010).
- [15] Wismüller, A., Vietze, F., and Dersch, D. R., “Segmentation with neural networks,” in [*Handbook of medical imaging*], 107–126, Academic Press, Inc. (2000).
- [16] Leinsinger, G., Schlossbauer, T., Scherr, M., Lange, O., Reiser, M., and Wismüller, A., “Cluster analysis of signal-intensity time course in dynamic breast MRI: does unsupervised vector quantization help to evaluate small mammographic lesions?,” *European radiology* **16**(5), 1138–1146 (2006).



- [17] Wismüller, A., Vietze, F., Behrends, J., Meyer-Baese, A., Reiser, M., and Ritter, H., “Fully automated biomedical image segmentation by self-organized model adaptation,” *Neural Networks* **17**(8-9), 1327–1344 (2004).
- [18] Hoole, P., Wismüller, A., Leinsinger, G., Kroos, C., Geumann, A., and Inoue, M., “Analysis of tongue configuration in multi-speaker, multi-volume MRI data,” (2000).
- [19] Wismüller, A., “Exploratory morphogenesis (XOM): a novel computational framework for self-organization,” *Ph. D. thesis, Technical University of Munich, Department of Electrical and Computer Engineering* (2006).
- [20] Wismüller, A., Dersch, D. R., Lipinski, B., Hahn, K., and Auer, D., “A neural network approach to functional MRI pattern analysis—clustering of time-series by hierarchical vector quantization,” in [*International Conference on Artificial Neural Networks*], 857–862, Springer (1998).
- [21] Wismüller, A., Vietze, F., Dersch, D. R., Behrends, J., Hahn, K., and Ritter, H., “The deformable feature map—a novel neurocomputing algorithm for adaptive plasticity in pattern analysis,” *Neurocomputing* **48**(1-4), 107–139 (2002).
- [22] Behrends, J., Hoole, P., Leinsinger, G. L., Tillmann, H. G., Hahn, K., Reiser, M., and Wismüller, A., “A segmentation and analysis method for MRI data of the human vocal tract,” in [*Bildverarbeitung für die Medizin 2003*], 186–190, Springer (2003).
- [23] Wismüller, A., “Neural network computation in biomedical research: chances for conceptual cross-fertilization,” *Theory in Biosciences* (1997).
- [24] Bunte, K., Hammer, B., Villmann, T., Biehl, M., and Wismüller, A., “Exploratory observation machine (XOM) with Kullback-Leibler divergence for dimensionality reduction and visualization.,” in [*ESANN*], **10**, 87–92 (2010).
- [25] Wismüller, A., Vietze, F., Dersch, D. R., Hahn, K., and Ritter, H., “The deformable feature map—adaptive plasticity for function approximation,” in [*International Conference on Artificial Neural Networks*], 123–128, Springer (1998).
- [26] Wismüller, A., “The exploration machine—a novel method for data visualization,” in [*International Workshop on Self-Organizing Maps*], 344–352, Springer (2009).
- [27] Wismüller, A., “Method, data processing device and computer program product for processing data,” (July 28 2009). US Patent 7,567,889.
- [28] Huber, M. B., Nagarajan, M., Leinsinger, G., Ray, L. A., and Wismüller, A., “Classification of interstitial lung disease patterns with topological texture features,” in [*Medical Imaging 2010: Computer-Aided Diagnosis*], **7624**, 762410, International Society for Optics and Photonics (2010).

- [29] Wismüller, A., “The exploration machine: a novel method for analyzing high-dimensional data in computer-aided diagnosis,” in [*Medical Imaging 2009: Computer-Aided Diagnosis*], **7260**, 72600G, International Society for Optics and Photonics (2009).
- [30] Bunte, K., Hammer, B., Villmann, T., Biehl, M., and Wismüller, A., “Neighbor embedding XOM for dimension reduction and visualization,” *Neurocomputing* **74**(9), 1340–1350 (2011).
- [31] Meyer-Bäse, A., Lange, O., Wismüller, A., and Ritter, H., “Model-free functional MRI analysis using topographic independent component analysis,” *International journal of neural systems* **14**(04), 217–228 (2004).
- [32] Wismüller, A., “A computational framework for nonlinear dimensionality reduction and clustering,” in [*International Workshop on Self-Organizing Maps*], 334–343, Springer (2009).
- [33] Meyer-Base, A., Auer, D., and Wismüller, A., “Topographic independent component analysis for fMRI signal detection,” in [*Proceedings of the International Joint Conference on Neural Networks, 2003.*], **1**, 601–605, IEEE (2003).
- [34] Meyer-Baese, A., Schlossbauer, T., Lange, O., and Wismüller, A., “Small lesions evaluation based on unsupervised cluster analysis of signal-intensity time courses in dynamic breast MRI,” *International journal of biomedical imaging* **2009** (2009).
- [35] Wismüller, A., Lange, O., Auer, D., and Leinsinger, G., “Model-free functional MRI analysis for detecting low-frequency functional connectivity in the human brain,” in [*Medical Imaging 2010: Computer-Aided Diagnosis*], **7624**, 76241M, International Society for Optics and Photonics (2010).
- [36] Meyer-Bäse, A., Saalbach, A., Lange, O., and Wismüller, A., “Unsupervised clustering of fMRI and MRI time series,” *Biomedical Signal Processing and Control* **2**(4), 295–310 (2007).
- [37] Huber, M. B., Nagarajan, M. B., Leinsinger, G., Eibel, R., Ray, L. A., and Wismüller, A., “Performance of topological texture features to classify fibrotic interstitial lung disease patterns,” *Medical Physics* **38**(4), 2035–2044 (2011).
- [38] Wismüller, A., Verleysen, M., Aupetit, M., and Lee, J. A., “Recent advances in nonlinear dimensionality reduction, manifold and topological learning,” in [*ESANN*], (2010).
- [39] Meyer-Baese, A., Lange, O., Wismüller, A., and Hurdal, M. K., “Analysis of dynamic susceptibility contrast MRI time series based on unsupervised clustering methods,” *IEEE Transactions on Information Technology in Biomedicine* **11**(5), 563–573 (2007).
- [40] Wismüller, A., Behrends, J., Hoole, P., Leinsinger, G. L., Reiser, M. F., and Westesson, P.-L., “Human vocal tract analysis by in vivo 3d MRI during phonation: a complete system for imaging, quantitative modeling,

and speech synthesis,” in [*International Conference on Medical Image Computing and Computer-Assisted Intervention*], 306–312, Springer (2008).

- [41] Wismüller, A., “Method and device for representing multichannel image data,” (Nov. 17 2015). US Patent 9,189,846.
- [42] Huber, M. B., Bunte, K., Nagarajan, M. B., Biehl, M., Ray, L. A., and Wismüller, A., “Texture feature ranking with relevance learning to classify interstitial lung disease patterns,” *Artificial intelligence in medicine* **56**(2), 91–97 (2012).
- [43] Wismüller, A., Meyer-Baese, A., Lange, O., Reiser, M. F., and Leinsinger, G., “Cluster analysis of dynamic cerebral contrast-enhanced perfusion MRI time-series,” *IEEE transactions on medical imaging* **25**(1), 62–73 (2005).
- [44] Twellmann, T., Saalbach, A., Muller, C., Nattkemper, T. W., and Wismüller, A., “Detection of suspicious lesions in dynamic contrast enhanced MRI data,” in [*The 26th Annual International Conference of the IEEE Engineering in Medicine and Biology Society*], **1**, 454–457, IEEE (2004).
- [45] Otto, T. D., Meyer-Baese, A., Hurdal, M., Summers, D., Auer, D., and Wismüller, A., “Model-free functional MRI analysis using cluster-based methods,” in [*Intelligent Computing: Theory and Applications*], **5103**, 17–24, International Society for Optics and Photonics (2003).
- [46] Varini, C., Nattkemper, T. W., Degenhard, A., and Wismüller, A., “Breast MRI data analysis by lle,” in [*2004 IEEE International Joint Conference on Neural Networks (IEEE Cat. No. 04CH37541)*], **3**, 2449–2454, IEEE (2004).
- [47] Huber, M. B., Lancianese, S. L., Nagarajan, M. B., Ikpot, I. Z., Lerner, A. L., and Wismüller, A., “Prediction of biomechanical properties of trabecular bone in mr images with geometric features and support vector regression,” *IEEE Transactions on Biomedical Engineering* **58**(6), 1820–1826 (2011).
- [48] Meyer-Base, A., Pilyugin, S. S., and Wismüller, A., “Stability analysis of a self-organizing neural network with feedforward and feedback dynamics,” in [*2004 IEEE International Joint Conference on Neural Networks (IEEE Cat. No. 04CH37541)*], **2**, 1505–1509, IEEE (2004).
- [49] Meyer-Baese, A., Lange, O., Schlossbauer, T., and Wismüller, A., “Computer-aided diagnosis and visualization based on clustering and independent component analysis for breast MRI,” in [*2008 15th IEEE International Conference on Image Processing*], 3000–3003, IEEE (2008).
- [50] Wismüller, A., Meyer-Bäse, A., Lange, O., Schlossbauer, T., Kallergi, M., Reiser, M., and Leinsinger, G., “Segmentation and classification of dynamic breast magnetic resonance image data,” *Journal of Electronic Imaging* **15**(1), 013020 (2006).

- [51] Bhole, C., Pal, C., Rim, D., and Wismüller, A., “3d segmentation of abdominal ct imagery with graphical models, conditional random fields and learning,” *Machine vision and applications* **25**(2), 301–325 (2014).
- [52] Nagarajan, M. B., Coan, P., Huber, M. B., Diemoz, P. C., Glaser, C., and Wismüller, A., “Computer-aided diagnosis in phase contrast imaging x-ray computed tomography for quantitative characterization of ex vivo human patellar cartilage,” *IEEE Transactions on Biomedical Engineering* **60**(10), 2896–2903 (2013).
- [53] Wismüller, A., Meyer-Bäse, A., Lange, O., Auer, D., Reiser, M. F., and Summers, D., “Model-free functional MRI analysis based on unsupervised clustering,” *Journal of Biomedical Informatics* **37**(1), 10–18 (2004).
- [54] Meyer-Baese, A., Wismüller, A., Lange, O., and Leinsinger, G., “Computer-aided diagnosis in breast MRI based on unsupervised clustering techniques,” in [*Intelligent Computing: Theory and Applications II*], **5421**, 29–37, International Society for Optics and Photonics (2004).
- [55] Nagarajan, M. B., Coan, P., Huber, M. B., Diemoz, P. C., Glaser, C., and Wismüller, A., “Computer-aided diagnosis for phase-contrast x-ray computed tomography: quantitative characterization of human patellar cartilage with high-dimensional geometric features,” *Journal of digital imaging* **27**(1), 98–107 (2014).
- [56] Nagarajan, M. B., Huber, M. B., Schlossbauer, T., Leinsinger, G., Krol, A., and Wismüller, A., “Classification of small lesions on dynamic breast MRI: Integrating dimension reduction and out-of-sample extension into cadx methodology,” *Artificial intelligence in medicine* **60**(1), 65–77 (2014).
- [57] Yang, C.-C., Nagarajan, M. B., Huber, M. B., Carballido-Gamio, J., Bauer, J. S., Baum, T. H., Eckstein, F., Lochmüller, E.-M., Majumdar, S., Link, T. M., et al., “Improving bone strength prediction in human proximal femur specimens through geometrical characterization of trabecular bone microarchitecture and support vector regression,” *Journal of electronic imaging* **23**(1), 013013 (2014).
- [58] Wismüller, A., Nagarajan, M. B., Witte, H., Pester, B., and Leistriz, L., “Pair-wise clustering of large scale Granger causality index matrices for revealing communities,” in [*Medical Imaging 2014: Biomedical Applications in Molecular, Structural, and Functional Imaging*], **9038**, 90381R, International Society for Optics and Photonics (2014).
- [59] Wismüller, A., Wang, X., DSouza, A. M., and Nagarajan, M. B., “A framework for exploring non-linear functional connectivity and causality in the human brain: mutual connectivity analysis (mca) of resting-state functional MRI with convergent cross-mapping and non-metric clustering,” *arXiv preprint arXiv:1407.3809* (2014).
- [60] Schmidt, C., Pester, B., Nagarajan, M., Witte, H., Leistriz, L., and Wismüller, A., “Impact of multivariate Granger causality analyses with embedded dimension reduction on network modules,” in [*2014 36th Annual International Conference of the IEEE Engineering in Medicine and Biology Society*], 2797–2800, IEEE (2014).

- [61] Wismüller, A., Abidin, A. Z., D'Souza, A. M., Wang, X., Hobbs, S. K., Leistriz, L., and Nagarajan, M. B., "Nonlinear functional connectivity network recovery in the human brain with mutual connectivity analysis (MCA): convergent cross-mapping and non-metric clustering," in [*Medical Imaging 2015: Biomedical Applications in Molecular, Structural, and Functional Imaging*], **9417**, 94170M, International Society for Optics and Photonics (2015).
- [62] Wismüller, A., Abidin, A. Z., DSouza, A. M., and Nagarajan, M. B., "Mutual connectivity analysis (MCA) for nonlinear functional connectivity network recovery in the human brain using convergent cross-mapping and non-metric clustering," in [*Advances in Self-Organizing Maps and Learning Vector Quantization*], 217–226, Springer (2016).
- [63] Schmidt, C., Pester, B., Schmid-Hertel, N., Witte, H., Wismüller, A., and Leistriz, L., "A multivariate Granger causality concept towards full brain functional connectivity," *PloS one* **11**(4) (2016).
- [64] Abidin, A. Z., Chockanathan, U., DSouza, A. M., Inglese, M., and Wismüller, A., "Using large-scale Granger causality to study changes in brain network properties in the clinically isolated syndrome (CIS) stage of multiple sclerosis," in [*Medical Imaging 2017: Biomedical Applications in Molecular, Structural, and Functional Imaging*], **10137**, 101371B, International Society for Optics and Photonics (2017).
- [65] DSouza, A. M., Abidin, A. Z., Leistriz, L., and Wismüller, A., "Exploring connectivity with large-scale Granger causality on resting-state functional MRI," *Journal of neuroscience methods* **287**, 68–79 (2017).
- [66] Chen, L., Wu, Y., DSouza, A. M., Abidin, A. Z., Wismüller, A., and Xu, C., "MRI tumor segmentation with densely connected 3d cnn," in [*Medical Imaging 2018: Image Processing*], **10574**, 105741F, International Society for Optics and Photonics (2018).
- [67] Abidin, A. Z., DSouza, A. M., Nagarajan, M. B., Wang, L., Qiu, X., Schifitto, G., and Wismüller, A., "Alteration of brain network topology in HIV-associated neurocognitive disorder: A novel functional connectivity perspective," *NeuroImage: Clinical* **17**, 768–777 (2018).
- [68] Abidin, A. Z., Deng, B., DSouza, A. M., Nagarajan, M. B., Coan, P., and Wismüller, A., "Deep transfer learning for characterizing chondrocyte patterns in phase contrast x-ray computed tomography images of the human patellar cartilage," *Computers in biology and medicine* **95**, 24–33 (2018).
- [69] DSouza, A. M., Abidin, A. Z., Chockanathan, U., Schifitto, G., and Wismüller, A., "Mutual connectivity analysis of resting-state functional MRI data with local models," *NeuroImage* **178**, 210–223 (2018).
- [70] Chockanathan, U., DSouza, A. M., Abidin, A. Z., Schifitto, G., and Wismüller, A., "Automated diagnosis of HIV-associated neurocognitive disorders using large-scale Granger causality analysis of resting-state functional MRI," *Computers in Biology and Medicine* **106**, 24–30 (2019).
- [71] Bellec, P., "COBRE preprocessed with NIAK 0.17 - lightweight release," (2016).

- [72] Abraham, A., Pedregosa, F., Eickenberg, M., Gervais, P., Mueller, A., Kossaifi, J., Gramfort, A., Thirion, B., and Varoquaux, G., “Machine learning for neuroimaging with scikit-learn,” *Frontiers in neuroinformatics* **8**, 14 (2014).
- [73] NIAK-pipeline, “<http://niak.simexp-lab.org/>,” (2019). Last accessed 19 August 2020.
- [74] Bellec, P., “Mining the hierarchy of resting-state brain networks: selection of representative clusters in a multiscale structure,” in [*2013 International Workshop on Pattern Recognition in Neuroimaging*], 54–57, IEEE (2013).
- [75] Kendall, M. G., “The treatment of ties in ranking problems,” *Biometrika* **33**(3), 239–251 (1945).
- [76] Suykens, J. A. and Vandewalle, J., “Least squares support vector machine classifiers,” *Neural processing letters* **9**(3), 293–300 (1999).